AIAA 80-1077R

Compact Diffusers for Centrifugal Compressors

L. W. Blair* and C. J. Russo†
General Electric Company, Lynn, Mass.

The smaller centrifugal compressor diameter of many advanced turbofan engines renders unattractive the use of conventional conical or channel diffusing systems to deliver low Mach number, low swirl flow to the combustor. A method has been developed for designing a set of low-diameter, radially-emanating, controlled-contour passage diffusers. Using this method, several such passages were designed and tested. Static pressure rise coefficients of 0.79-0.82 were obtained at throat blockages of 2-3% for an inlet Mach number of 0.7-0.8 and an exit Mach number of 0.10 with 5-10 deg of residual swirl within an outer diameter 20% smaller than conventional engines.

Nomenclature

a	= semimajor axis
A	= throat area
b	= semiminor axis
B_t	= throat blockage
C_p	= static pressure rise coefficient
e_m, e_n	= cross-section exponents
L	= true centerline length
L_t	= total true centerline length
m	= meridional distance
M	= Mach number
P_{cell}	= cell atmospheric pressure
P_s	= throat static pressure
$P_{T_{\text{in}}}$	= inlet supply pressure
Re_d	= throat Reynolds number
T_T	= inlet total temperature
W	= weight flow
x	= cross-section abscissa
X	= rectangular coordinate
y	= cross-section ordinate
Y	= rectangular coordinate
Z	= axial coordinate
β	= passage centerline angle
θ	= wrap angle

I. Introduction

THE application of centrifugal compressors in turboshaft and turbofan engines may require small diffuser diameters for lower weight and smaller frontal area. Conventional passage diffusers of circular or rectangular cross-section typically have large outlet diameters for exit Mach numbers below 0.20. The objective of this reported project was to lower the compressor diameter by wrapping the diffusing passages around a radial-to-axial turn while maintaining a high level of diffuser performance. This approach avoids dumping the flow into an annular turning duct with significant mixing and Mach number losses. The test program presented herein evaluated some of the design variables which were deemed most significant in affecting passage performance. These designs considered potential engine applications in the choice of the range of parameters studied. A requirement in these designs was the delivery of a low outlet Mach number (0.10) and swirl (0-15 deg) into a combustor plenum.

Presented as Paper 80-1077 at the AIAA/SAE/ASME 16th Joint Propulsion Conference, Hartford, Conn., June 30-July 2, 1980; submitted Aug. 8, 1980; revision received March 30, 1981.

*Manager, T700 and Advanced Centrifugal Aerodynamic Design.
†Engineer, Aerodynamic Design and Analysis.

The design of the low-diameter diffusers utilized an analytical model to generate the passages which permitted a direct interface with interactive graphics (IAG) to generate the detailed design definition. This analytical definition also allowed a systematic set of design variables to be independently evaluated. These designs are called controlled-contour passages because the flowpath is defined by a smooth analytical function. The cross-sectional shape of these passages can be smoothly varied (i.e., from circular to elliptic to rectangular). This analytic procedure is applied herein to centrifugal compressors but is general and can be used to define other shapes (i.e., engine inlets and external bodies).

In the present study, the performance of the controlled-contour diffuser passages were evaluated experimentally by blowing air through individual scaled-up passages varying throat blockage and Mach number over the range encountered in engine conditions. Evaluating diffuser performance from single passage blow tests does not include the effects of physical size, throat Reynolds number, nonuniform inlet velocity profiles, and high inlet turbulence levels. The effects of the larger diffuser physical size and smaller throat Reynolds number on diffuser performance were investigated and reported in Ref. 1. In the study reported in Ref. 1, nonuniform inlet velocity profiles and high inlet turbulent intensities which are encountered in engine environments but not simulated in the blow tests were found to effect only the internal distribution of static pressure rise. The overall diffuser performance aft of the throat was found to be a function only of throat blockage, Mach number, and Reynolds number. Thus the single passage blow tests permitted the optimization of the controlled-contour diffuser designs and

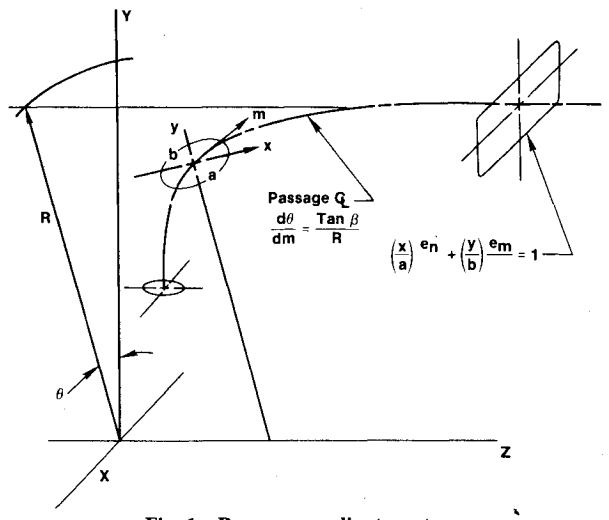

Fig. 1 Passage coordinate system.

also allowed detailed static pressure measurements and exit traverse surveys which are difficult to acquire in centrifugal stage tests.

II. Diffuser Design

A general approach for designing curved ducts in space was defined which permitted independent specification of turning, area change, and cross-sectional shape. This design procedure required a definition of the passage centerline in space and a passage area distribution along this centerline. The passage inlet cross section can be either circular or rectangular for either a conical or channel diffuser discharge. In the test series presented herein, circular inlet cross sections were investigated. The projection in the meridional plane of the passage centerline was an ellipse for all designs in this study (see Fig. 1). The ellipse aspect ratio (minor axis/major axis) was 0.666 with the major axis 0.75 times the inlet cross-section diameter. The centerline projection was continued in a straight line two inlet diameters downstream of the end of the ellipse. Coordinates of the centerline in space can be calculated from the coordinates in the meridional plane, using the relationship for passage wrap angle given in the following equation:

$$\frac{d\theta}{dm} = \frac{\tan\beta}{R} \tag{1}$$

The meridional distance m is the length of the projected passage centerline on the R-Z plane. The passage centerline angle β determined the direction cosines of a plane which contained the passage cross sections and is distributed uniformly to avoid excessive rates of turning. This equation has proved useful in the definition of radial turbomachinery geometry and is discussed in Ref. 2. In this application, the passage centerline angle β represents a mean flow angle. The distribution of this angle controls the rate of turning of the passage where the fluid is turned from a radial to an axial flow direection while removing about 50-60 deg of swirl.

The passage cross sections are generated from the following equation:

$$(x/a)^{e_n} + (y/b)^{e_m} = 1 \tag{2}$$

The exponents e_m and e_n determine the "rectangularity" of the perimeter or the "sharpness" of the corners from the value 2 (ellipse) to 8 or more (rectangular with corner fillet). The constants a and b are the semimajor and semiminor axes of the cross section, as shown in Fig. 1. The centrifugal compressor diffuser passage had the semiminor axis on a radial line, and the semimajor axis was an arc for an annular passage discharge. The aspect ratio of the passage a/b is adjusted to have at least twice the nominal wall thickness between adjacent passages.

The design procedure using Eqs. (1) and (2) provided an analytic definition of the entire duct. The design approach used high diffusion rates in the initial radial section to minimize the Mach number into the radial-to-axial turn. The selected diffusion rate was below the transitory stall boundary for the expected 2-3% blockage in engine applications. The passage cross section was transformed from circular to elliptic before the radial-to-axial turn in order to reduce the turning losses. The deswirl process was initiated near the exit of the radial-to-axial turn. Passage cross sections were generated to be displayed on interactive graphics (IAG) and to prepare templates for fabrication of test hardware.

The test program evaluated various design parameters in a series of test configurations. These parameters were the 1) rate of radial-to-axial turn; 2) inlet Mach number into radial-to-axial turn; 3) circumferential deswirl rate and the initial location of deswirling; 4) effect of passage splitters; 5) rate of passage area increase; and 6) number of diffuser passages.

A 6½-deg cone was also fabricated to obtain baseline data for comparison with other available test results and to verify the adequacy of the test apparatus.

The six test models reported herein had the deswirl distributions shown in Fig. 2 and the area distributions shown in Fig. 3. The Mach number into the radial-to-axial turn was 0.46 for designs 1, 2, and 4; 0.41 for design 3, and 0.27 for designs 5 and 6. The designs 1-5 subtended an arc equivalent to 33 diffuser passages and design 6 was 25 passages. These designs were tested with and without a splitter vane in the exit region of the diffuser passage. In all designs tested the splitter was placed in the center of the passage with the leading edge at the exit of the radial-to-axial turn and extended over about 45% of the true centerline length. Because of the large number of design parameters, the ranges explored in this initial test series were values deemed more significant for engine applications.

In constructing the test series, designs 1 and 2 were identical except that design 2 was shortened to have 15 deg of residual swirl. Design 3 had a higher initial rate of area increase, but was identical to design 1 in other parameters. Design 4 had a deswirl distribution which decreased the rate of turning near the exit. Designs 5 and 6 had a higher initial rate of area increase similar to design 3 and evaluated the effect of 33 vs 25

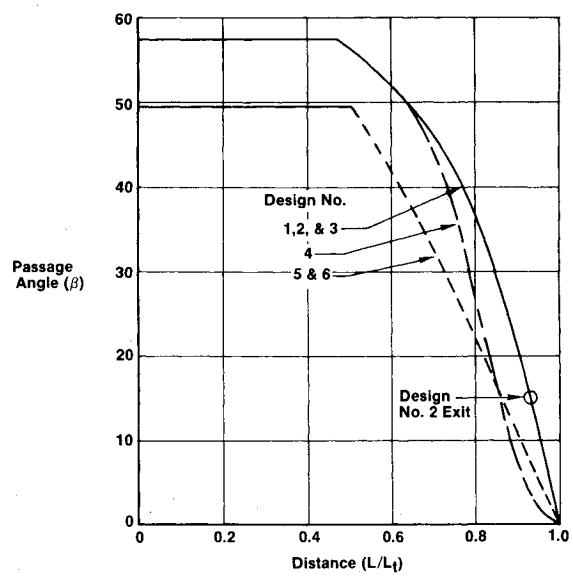

Fig. 2 Deswirl angle distribution.

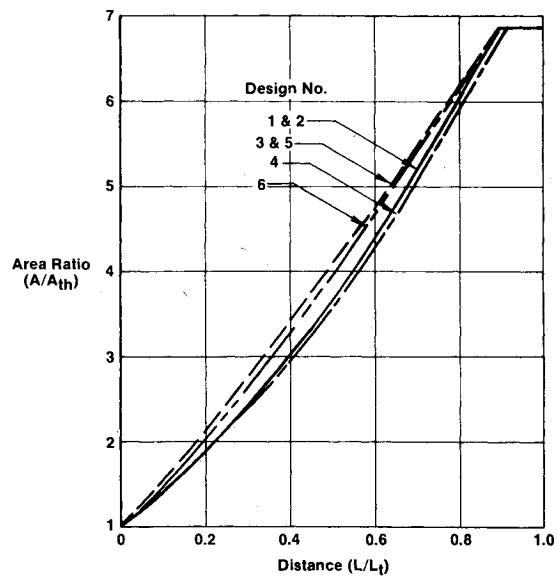

Fig. 3 Passage area distribution.

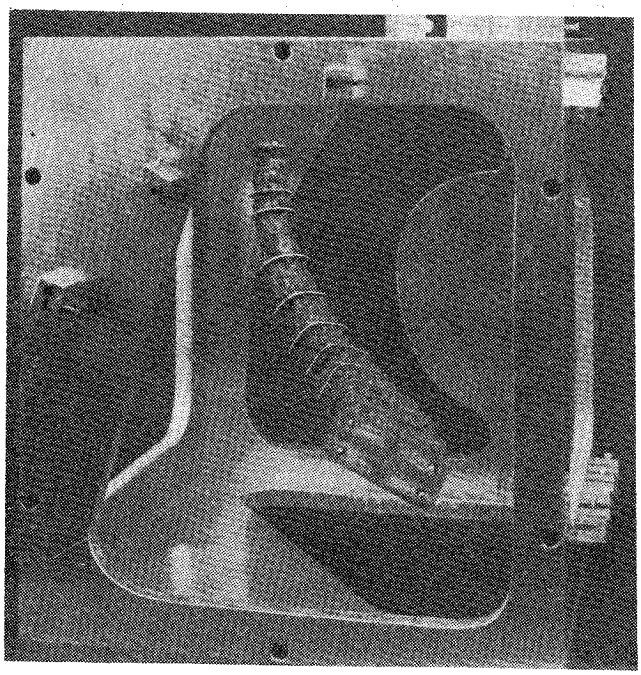

Fig. 4 Strung box with cross section.

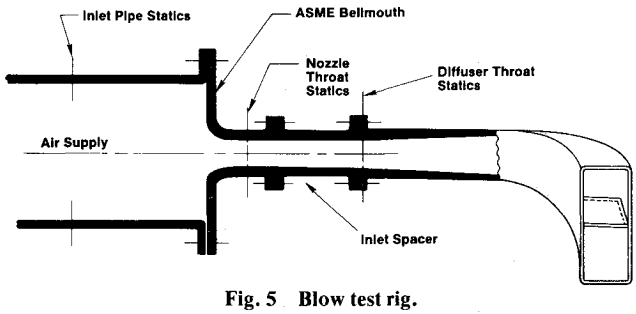

Fig. 5 Blow test rig.

passages. The initial passage centerline angle was 49.6 deg for designs 5 and 6, since it was closer to a proposed engine application.

III. Test Apparatus

The test models were constructed using a strung box technique to position the various cross sections. This method enclosed the test section with a box, and the axes of each cross section were extended until they intercepted the inner walls of the box. The intercept points were determined on the IAG system, along with templates for manufacture of the box. A pair of fine wires were strung for each section, as shown in Fig. 4. The wire diameter was considered in determining the intercept points. The sections were tied together and the master passage was built up to form a smooth surface. This passage was reproduced in plaster to form a core for a fiberglass test section. The model was molded with integral static pressure taps positioned at each cross section. Four static pressure taps were used at each measurement plane: top, bottom, and each side wall.

The blow test apparatus for these diffuser tests is shown in Fig. 5 for a typical setup. The inlet section was an elliptic-shaped ASME nozzle which provided an additional airflow measurement. Attached to the test section was a set of inlet spacers which were used to vary the initial boundary-layer blockage into the test sections with the longest spacer 4 in. long. The inlet diameter was 0.80 in.

A hot-film X probe was used to measure the flow velocity and angle at the passage exit. The hot-film probe was a TSI model 1240-60 cross-flow X probe which was calibrated for velocity and angle. This probe was set at various immersions

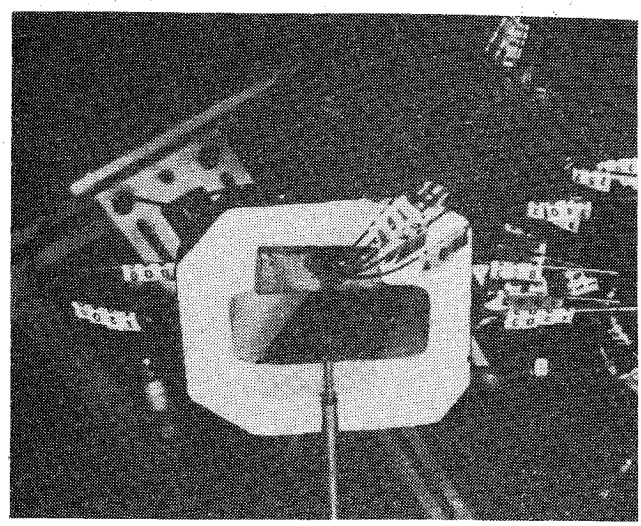

Fig. 6 Blow test rig with hot-film probe.

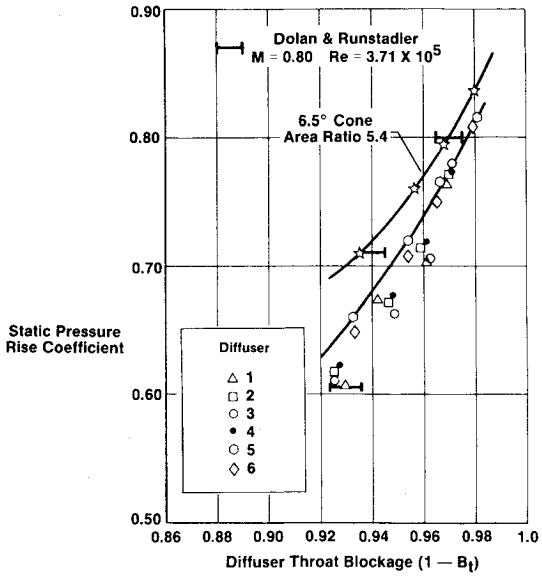

Fig. 7 Diffuser performance vs throat blockage at $Re_d = 4.3 \times 10^5$ and $M = 0.80$.

and traversed across the passage to determine the flow profile. The hot-film probe is shown in position in Fig. 6.

IV. Test Results and Analysis

A straight, 6½-deg cone was the first diffuser blow-tested in order to verify the symmetry of the flow entering the diffuser and to verify the calculated blockage which assumed no total pressure loss from the inlet-pipe static pressure taps to the diffuser-throat static pressure taps (see Fig. 5). Thus at the diffuser throat the total pressure, static pressure, weight flow, geometric area, and temperature are known, and the Mach number and blockage can be calculated from compressible flow equations, assuming no circumferential flow component exists. This calculation procedure is identical to that of Dolan and Runstadler (Ref. 3) and the blow-test measured static pressure rise coefficient is in excellent agreement with their measured results, as shown in Fig. 7. The error bars on the Dolan and Runstadler data reflect the variation in blockage given in their report.

As in the Dolan and Runstadler study, the controlled-contour diffuser performance was measured as a function of throat Mach number with each inlet spacer (but at only one Reynolds number). Figure 8 shows typical results. Hidden in these results is any variation of throat blockage with throat

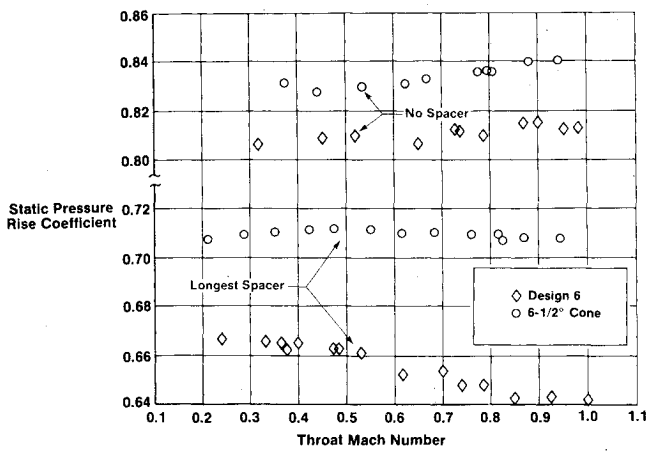

Fig. 8 Typical variation of C_p vs throat Mach number.

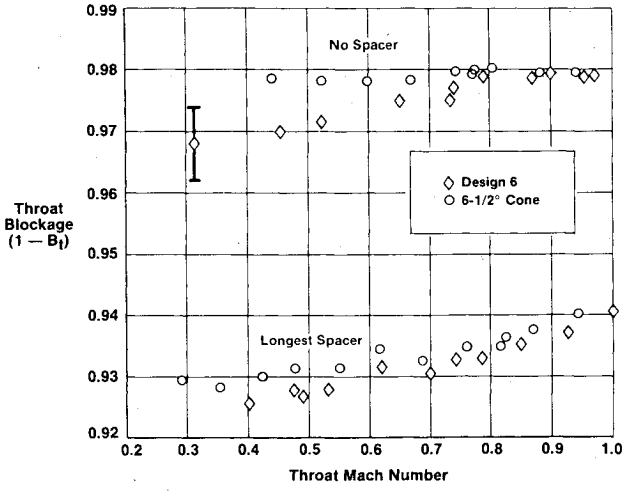

Fig. 9 Variation of throat blockage with Mach number.

Mach number. Figure 9 shows that throat blockage is very nearly constant with Mach number for no inlet spacer but does decrease by 1% for the longest inlet spacer as the higher flow rates thin out the approaching boundary layers. Figures 8 and 9 imply that the controlled-contour diffusers degrade slightly in performance with increasing throat Mach number, despite the decreasing boundary layer blockage.

The controlled-contour diffusers have been rated at a fixed throat Mach number of 0.80 which is typical of engine applications. Shown in Fig. 7 is the overall static pressure rise of the controlled-contour diffusers tested at a throat Mach number of 0.80 and $Re_d = 4.3 \times 10^5$. The greater scatter in calculated throat blockage for designs 1-5 reflect the poorer throat static tap quality obtained in the plaster models. Design 6 had a metal throat region, much better tap quality, and thus much reduced scatter in the calculated throat blockage. The error analysis on blockage and C_p is given in the Appendix and indicates that the differences in C_p are significant between the last two designs and the first four designs.

A clearer ranking of the performance of these six designs is given by the total-to-static pressure loss measured for each design, since the total pressure loss, $(P_{T_{in}} - P_{cell})/P_{T_{in}}$, is much less sensitive to throat blockage. This loss for all designs is given in Fig. 10 as a function of throat blockage. The one throat blockage number given is that calculated with design 6 which had the best throat static taps. This loss data clearly ranks the designs in the order 5, 6, 3, 2, 4, 1—from best to worst for blockages around 2-3%. All of the results shown in Figs. 7 and 10 are without an exit splitter.

The effect of an exit splitter is shown in Fig. 11 for designs 5 and 6. The flow conditions are again $Re_d = 4.3 \times 10^5$ and $M = 0.80$. The differences in C_p are larger than experimental

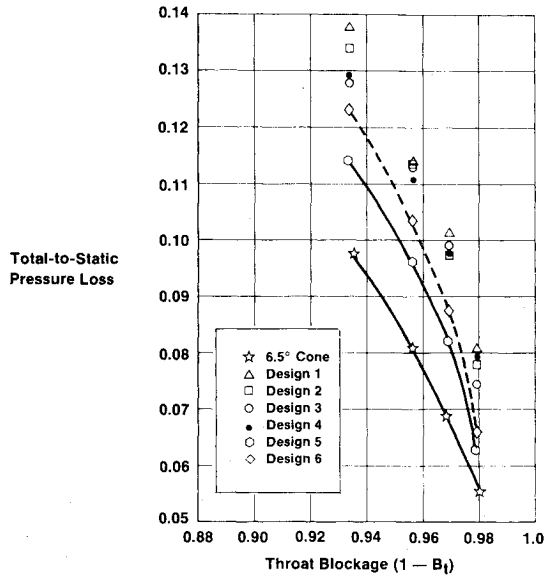

Fig. 10 Total pressure loss vs blockage.

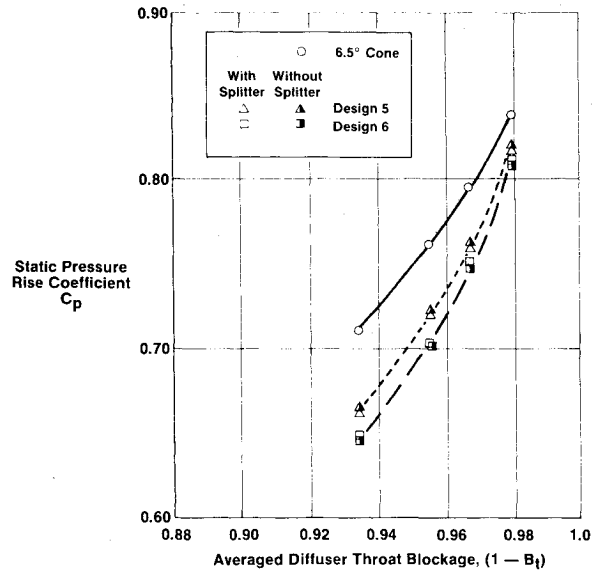

Fig. 11 Effect of an exit splitter on diffuser performance.

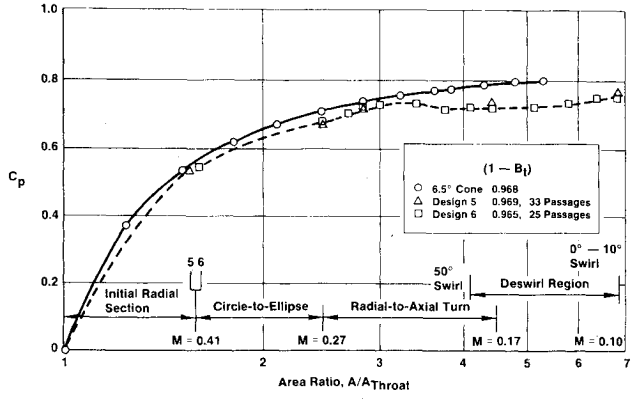

Fig. 12 Static pressure rise distribution within the controlled-contour diffuser at $Re_d = 4.3 \times 10^5$ and $M = 0.80$.

uncertainty and show slight gains or losses in C_p with a splitter, depending on the design. However, the differences are judged too small to justify the added expense and increased manufacturing difficulty of adding splitters in the designs tested.

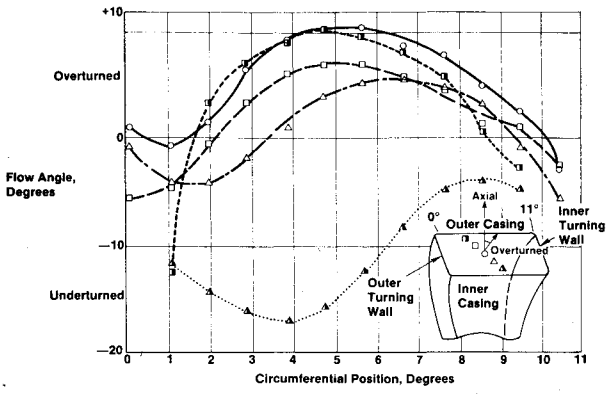

Fig. 13 Survey of exit Mach number for design 6 at 3% throat blockage and $M=0.80$.

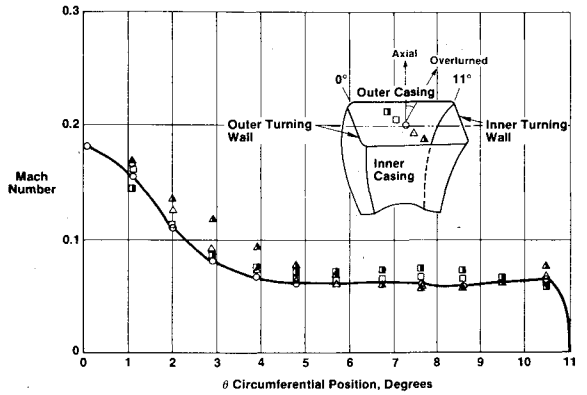

Fig. 14 Survey of exit flow angle for design 6 at 3% throat blockage and $M=0.80$.

The distribution of static pressure rise within the controlled contour diffusers is shown in Fig. 12. Unlike the 6½-deg cone where C_p increases monotonically, the controlled-contour diffusers experienced a slight decrease in C_p and a subsequent nearly constant C_p region about midway through the radial-to-axial turn. Increasing differences appeared among the four static taps at each cross section, indicating significant secondary flows existed. The differences in static pressure are consistent for all designs and were at maximum 0.5% of the average exit static pressure. The four static pressures at each section were arithmetically averaged to obtain the C_p for that cross section. A further increase of about 3% in C_p occurred in the final 13% of area increase, although the differences in static pressure on the inner- and outer-turning walls persisted.

To quantify the implied regions of high and low flow, detailed surveys of velocity and flow angle at the diffuser exits of designs 5 and 6 were taken with the hot-film X-probe described in the apparatus section. The surveys were done without an exit splitter. The circumferential distributions of Mach number and flow angle are given in Figs. 13 and 14 for design 6 at 3% throat blockage and a throat Mach number of 0.80. There is clearly a high momentum region near the outer-turning wall. In addition, the secondary flows tended to overturn the bulk of the flow except very near the inner casing. The rather large amount of overturning measured results from the relatively large influence small secondary flows can have at the low exit Mach number levels of the discharge flow. Because of the low momentum level of the discharge flow, the large changes in discharge angle do not substantially affect the combustor pattern factor. Similar results were obtained for the other three throat blockages and for design 5.

V. Conclusions

A comparison of the basic design geometries given previously and the test results shown in Figs. 7 and 10 leads to the following conclusions:

1) It is important to reduce the Mach number into the radial-to-axial turn as much as possible without placing the inlet cone in a region of transitory stall.

2) The deswirling distributions of designs 4-6 produce more gradual turning rates and raise C_p, especially at higher throat blockages (see designs 1 and 4).

3) Leaving 15 deg of exit swirl does raise the C_p (see designs 1 and 2).

4) The best performing designs (3, 5, and 6) had higher initial rates of area increase (see Figs. 3 and 10).

5) The pressure of a splitter vane at the diffuser exit does not substantially affect the C_p obtained (see Fig. 11) at least for the splitter geometry in this experiment.

6) Decreasing the number of diffuser passages decreases performance due to higher passage curvatures (see designs 5 and 6).

In addition to the above conclusions, it can be noted that like other more geometrically simpler diffusers, the performance of the controlled-contour diffuser is primarily a function of throat blockage. It also appears to be true that at throat blockages larger than 2-3% the controlled-contour diffuser performance degrades with increasing throat Mach number more rapidly than conical diffusers. Since in most centrifugal compressor applications the throat Mach number does not vary widely, this increased sensitivity is not an important problem in the design of such a diffuser.

Finally, it is clear that controlled-contour diffusers can be quickly and inexpensively designed and tested for a specific application, using the methods presented in this paper. These diffusers have been shown to achieve state-of-the-art static pressure rise coefficients of 0.79-0.82 at throat blockages of 2-3% and to produce at their exits low Mach numbers near 0.10 and 0 swirl. All of this performance can be achieved within an outer diameter significantly smaller than conventional engines.

Appendix: Error Analysis

An error analysis has been performed on the parameters C_p, $\Delta P_T/P_T$, B_t, and M calculated from the measured test variables. In each case, the uncertainty of the parameter was defined to be equal to the root mean square of uncertainties in the measurement quantities where each is weighted by the appropriate derivative. Thus if $g=g\ (X_1,X_2,X_3,..,X_n)$, then the error in g is given by

$$\Delta g=\left\{\sum_i\left(\frac{\partial g}{\partial x_i}\Delta x_i\right)^2\right\}^{1/2}$$

where ΔX_i is the random error in the measured quantity X_i and all of the X_i's are independent.

Thus the error in g is a function of not only the errors X_i but also the absolute level of the measured quantities. Since all C_p and B_t were quoted for a throat Mach number of 0.80, the error analysis for these two parameters was calculated at that flow condition. The error in $\Delta P_T/P_T$ and M was calculated for both $M=0.4$ and 0.80 and the worst case quoted. The errors were calculated using the following estimated errors in measured quantities:

P_{cell} = cell atmospheric pressure = ±0.003 psi
$P_{T_{\text{in}}}$ = inlet pipe supply pressure = ±0.008 psi

Table A1 Calculated uncertainties[a]

C_p	±0.002	0.2%
$\Delta P_T/P_T$	±0.0005	0.6%
B_t	±0.006	0.6%
M	±0.005	0.65%

[a] On plots where the symbol size is not indicative of these errors, error bars are noted.

P_{s_*} = throat static pressure = ±0.02 psi for plaster inlet, = ±0.01 psi for metal inlet
W = airflow rate = ±0.001 pps
T_T = inlet supply temperature = ±1.60° F
A = throat area = ±0.001 in.

These estimated errors reflect instrumentation quality as well as the accuracy of the measuring equipment itself. These errors resulted in the following calculated uncertainties found in Table A1.

References

[1] Russo, C.J. and Blair, L.W., "Effect of Size and Reynolds' Number on Centrifugal Diffuser Performance," ASME Paper 81-GT-8, March 1981.

[2] Katsanis, T., "Use of Arbitrary Quasi-Orthogonals for Calculating Flow Distribution in the Meridional Plane of a Turbomachine," NASA TN D-2546, Dec. 1964.

[3] Dolan, F.X. and Runstadler, P.W., "Pressure Recovery Performance of Conical Diffusers at High Subsonic Mach Numbers," NASA CR-2299, Aug. 1973.